Journal of Power Sources 196 (2011) 4499–4505

Contents lists available at ScienceDirect

Journal of Power Sources

journal homepage: www.elsevier.com/locate/jpowsour

Pt support of multidimensional active sites and radial channels formed by SnO_2 flower-like crystals for methanol and ethanol oxidation

Hulin Zhang [a], Chenguo Hu [a,*], Xiaoshan He [a], Liu Hong [b], Guojun Du [b], Yan Zhang [a]

[a] Department of Applied Physics, Chongqing University, 174 Shapingba Street, Chongqing 400044, PR China
[b] State Key Laboratory of Crystal Materials, Shandong University, Jinan 250100, PR China

ARTICLE INFO

Article history:
Received 19 November 2010
Received in revised form
27 December 2010
Accepted 7 January 2011
Available online 19 January 2011

Keywords:
Tin dioxide
Platinum catalyst
Electrooxidation
Methanol
Ethanol

ABSTRACT

SnO_2 nanoflowers and nanorods have been synthesized by the hydrothermal method without using any capping agent. Both types of SnO_2 nanostructures are selected as a support of Pt catalyst for methanol and ethanol electrooxidation. The synthesized SnO_2 nanostructures and SnO_2 supported platinum (Pt/SnO_2) catalysts are characterized by X-ray diffraction, scanning electron microscope and high resolution transmission electron microscope. The electrocatalytic properties of the Pt/SnO_2 and Pt/C catalysts for methanol and ethanol oxidation have been investigated systematically by typical electrochemical methods. The influence of SnO_2 morphology on its electrocatalytic activity is comparatively investigated. The Pt/SnO_2 flower-shaped catalyst shows higher electrocatalytic activity and better long-term cycle stability compared with other electrocatalysts owing to the multidimensional active sites and radial channels of liquid diffusion.

1. Introduction

Direct alcohol fuel cells (DAFCs) based on liquid fuels have attracted considerable interest as compact electrochemical power source for portable electronic devices and fuel cell vehicles owing to their much higher energy density than gaseous fuels. Contrary to secondary batteries, DAFCs can supply continuous power as long as methanol or ethanol is provided. Direct injection of alcohol fuel would not has the problems of the production, purification and storage of hydrogen. Among several small organic molecules, methanol can be more efficiently oxidized than other alcohols, and ethanol is one of the most promising fuels with its low toxicity, abundance, low permeability (but not negligible) across proton exchange membrane [1,2] and higher energy density (1325.31 kJ mol^{-1}) than that of methanol (702.32 kJ mol^{-1}) [3]. However, the practical application of DMFCs is still a matter of concern because of the low activity of anodic catalysts and the use of precious platinum [4]. To improve the electrocatalytic activity of anodes and to reduce the catalyst cost, recently, a lot of work has been carried out to develop new anodic catalysts. One approach to cost reduction is to use the Pt-based alloys or oxides [5–9], and another way is to efficiently utilize Pt by distributing limited Pt nanostructures on a novel support [10,11].

Previous studies showed that tin oxide in the vicinity of Pt nanoparticles could enable oxygen species conveniently to remove the CO-like residues from oxidation of ethanol to free Pt active sites [12], and carbon-supported Pt/SnO_2 catalyst exhibits surprising promotion of catalytic activity for ethanol electrooxidation [13]. Very recently, Pt/Sn catalyst supported on SnO_2 nanowires has been demonstrated to be able to enhance the activities of both methanol and ethanol oxidation, with a more pronounced effect on the oxidation current of ethanol [14]. Although there is a wide agreement that Pt/SnO_2 is active for the oxidation of methanol and ethanol, it is necessary to have a better understanding of the roles of SnO_2 support with different morphologies. Besides, the reported SnO_2 supports are commonly of nanoparticles or nanowires. Specific structure such as flower-like nanostructure consisting of dense nanorods as a Pt support of DAFCs has not been reported yet.

Herein, SnO_2 nanoscrystals with different morphologies have been synthesized by the hydrothermal method, which are used as supports for the load of Pt nanocatalysts to assist a complete oxidation of methanol/ethanol. The morphology of SnO_2 nanostructures and Pt/SnO_2 catalysts are characterized by X-ray diffraction (XRD), field emission scanning electron microscope (FESEM), energy-dispersive X-ray spectroscope (EDS) and high resolution transmission electron microscope (HRTEM). In addition, due to high stability of SnO_2 in diluted acidic solution, the performances of the SnO_2 supported Pt catalysts (Pt/SnO_2) for methanol and ethanol electrooxidation are studied via cyclic voltammetry

* Corresponding author. Tel.: +86 236 510 4741; fax: +86 236 511 1245.
E-mail addresses: hucg@cqu.edu.cn, hu_chenguo@yahoo.com (C. Hu).

0378-7753/$ – see front matter © 2011 Elsevier B.V. All rights reserved.
doi:10.1016/j.jpowsour.2011.01.030

(CV), linear sweep voltammetry (LSV) and chronoamperometry in acidic medium.

2. Experimental

2.1. Chemicals

$SnCl_4{\cdot}5H_2O$, NaOH, $Na_2SO_4{\cdot}10H_2O$, NaF, $NaBH_4$, methanol, ethanol, $H_2PtCl_6{\cdot}6H_2O$ and H_2SO_4 were purchased from Chongqing Chemical Reagent Company. Carbon black (Vulcan XC72R) was from CABOT Corp. Nafion and silver paste were purchased from Sigma–Aldrich and SPI Supplies. All chemicals were of analytical grade and were used as received. Deionized water was used throughout.

2.2. Synthesis of SnO_2 nanocrystals

Flower-like SnO_2 nanostructures were synthesized by the hydrothermal method. In a typical reaction: (1) 0.324 g NaOH, 0.263 g $SnCl_4{\cdot}5H_2O$, 0.17 g $Na_2SO_4{\cdot}5H_2O$ and 10 mL deionized water were put in a beaker. (2) After stirring for about 5 min, absolute ethanol (10 mL) was added into the reaction mixture to obtain a white translucent suspended solution, which was then transferred into a 25 mL Teflon-lined autoclave. (3) The vessel was sealed and put in a furnace preheated to 180 °C. (4) After reacting for 24 h, the vessel was taken out and let cool down to room temperature naturally. (5) The blue product was washed with deionized water and ethanol several times. The SnO_2 nanorods were obtained in the same steps besides taking 0.03 g NaF instead of $Na_2SO_4{\cdot}5H_2O$ in step (1).

2.3. The preparation and characterization of Pt/SnO_2 catalysts

The SnO_2 nanocrystals (0.038 g) and $H_2PtCl_6{\cdot}6H_2O$ (0.0088 g) and 5 mL deionized water were put in a 25 mL beaker. After that, 0.022 mol/L $NaBH_4$ solution was dropped into the solution, and then the solution was under continuous magnetic stirring until the color of the solution remained unchanged. Finally, the black product was washed with deionized water and ethanol several times.

X-ray powder diffraction (XRD) was taken to identify the crystalline phase of the as-prepared samples in a continuous mode over the range of 20–80°. Cu was used as the source of X-ray. The morphology of SnO_2 nanostructures and the Pt/SnO_2 nanostructures were characterized by FESEM (Nova 400 Nano SEM), TEM (TEM, JEOL4000EX) and HRTEM (HRTEM 400 kV, JEOL4000EX).

2.4. Electrode fabrication and electrochemical measurements

The graphite (*G*, 10 mm × 10 mm × 4 mm in length, width and thickness) electrode was polished, and then rinsed thoroughly with deionized water, and finally sonicated in deionized water for 1 min. After drying in air, the graphite electrode was coated by 10 μL dispersed Pt/SnO_2 ethanol solution, and then allowed to dry under an infrared lamp. To immobilize the Pt/SnO_2 nanostructures on the graphite electrode and to improve the anti-interference ability, 4 μL of 0.5 wt% Nafion was dropped on the surface of the electrode. Finally, the edges and back of the electrodes were covered by epoxy resin leaving an open area of 5 × 5 mm. The obtained electrodes were referred as Pt/SnO_2/G electrode. The Pt loading on each electrode was 0.14 mg cm^{-2}. To compare catalysis of the Pt/SnO_2 electrocatalysts with other common Pt-based catalyst, Pt supported on carbon black (Pt/C) was prepared as the reported [15] with the same loading of 0.14 mg cm^{-2} Pt.

LK98B(II) and CHI600C electrochemical analyzer was employed for electrochemical measurements, which were carried out with a conventional three-electrode electrochemical cell. Pt foil and Ag/AgCl (saturated KCl) were used respectively as the counter and reference electrodes. All the experiments were performed at room temperature (20 °C).

3. Results and discussion

3.1. Characterization of the as-prepared SnO_2 and Pt/SnO_2 nanostructures

XRD patterns of the SnO_2 samples obtained in different conditions are shown in Fig. 1A. All the peaks can be indexed to the tetragonal phase of SnO_2 (JCPDS 41-1445), and no peaks of impurities are detected, indicating that the SnO_2 samples are pure and well crystallized.

Fig. 1B and C shows typical SEM images of the sample synthesized with Na_2SO_4, indicating the flower-shaped structure like snow cone (inset C) with size of 3 μm consisting of dense SnO_2 nanorods with typical length around 1 μm and diameter of 200 nm. The nanorods gathered together, rooted in one centre and assembled into the beautiful flower-like morphology. TEM and electron diffraction pattern (inset B) demonstrate the single crystal structure of the nanorod. Fig. 1D and E shows the typical SEM images of the sample synthesized with NaF, which illustrate that the obtained product is of SnO_2 nanorods with length of 1.5 μm and diameter of 300 nm. EDS (inset C) shows that the SnO_2 nanocrystals contain elements of tin and oxygen. We find that the reaction time and temperature cannot change the morphology of elementary parts (rods). SO_4^{2-} induces the SnO_2 nanorods to assemble into flowers, but F^- cannot.

After being deposited by Pt, the SnO_2 nanostructures are covered by Pt nanoparticles. Fig. 2A shows XRD patterns of the Pt/SnO_2 (flower) catalyst and Pt/SnO_2 (rod) catalyst. Almost all the peaks can be indexed to the tetragonal phase of SnO_2 (JCPDS 41-1445), except that one peak of Pt (JCPDS 88-2343) is detected as an evidence of successful Pt coating on the SnO_2 nanostructures. Fig. 2B and C shows typical EDS results of the obtained Pt/SnO_2 nanostructures, further revealing that the samples contain Pt in addition to tin and oxygen. The FESEM images of the Pt/SnO_2 (flower) catalyst and Pt/SnO_2 (rod) catalyst are shown in Fig. 2D and E respectively. The details of the Pt/SnO_2 catalysts are shown by TEM image in Fig. 2F and HRTEM image in Fig. 2G, respectively, which suggest a lot of Pt nanocrystals with sizes ranging from 5 to 10 nm distribute uniformly onto the surface of SnO_2 nanorods.

3.2. Electrooxidation of methanol and ethanol on the Pt/SnO_2/G and Pt/C/G electrodes

The CVs taken in 0.5 M H_2SO_4 for the Pt/SnO_2 (flower)/G, Pt/SnO_2 (rod)/G and Pt/C/G electrode (with same geometric area) are shown in Fig. 3A. In the acid medium, there are two hydrogen desorption peaks at −0.103 V and 0.035 V in positive scan and reduction peak at 0.522 V in negative scan for the two Pt/SnO_2/G electrodes. Obviously, the peaks on the Pt/SnO_2 (flower)/G electrodes are much stronger than that on the Pt/SnO_2 (rod)/G and Pt/C/G electrode, which suggests the Pt/SnO_2 (flower) catalyst has better catalytic activity. The electrochemical active surface (EAS) is calculated according to the area of hydrogen adsorption/desorption peaks [16]. The EAS is 83.2 $m^2\,g^{-1}$ for Pt/SnO_2 (flower), 41.7 $m^2\,g^{-1}$ for Pt/C and 31.1 $m^2\,g^{-1}$ for Pt/SnO_2 (rod) in acidic media, indicating an effective catalysis due to the multidimensional structure of the Pt/SnO_2 (flower) catalyst.

Fig. 3B and C shows the CVs of the methanol (Fig. 3B) and ethanol (Fig. 3C) electrooxidation on the Pt/SnO_2/G electrodes and Pt/C/G electrode in acid medium. To make comparison clearer, current densities are calculated by the specific mass of the loading of Pt. The

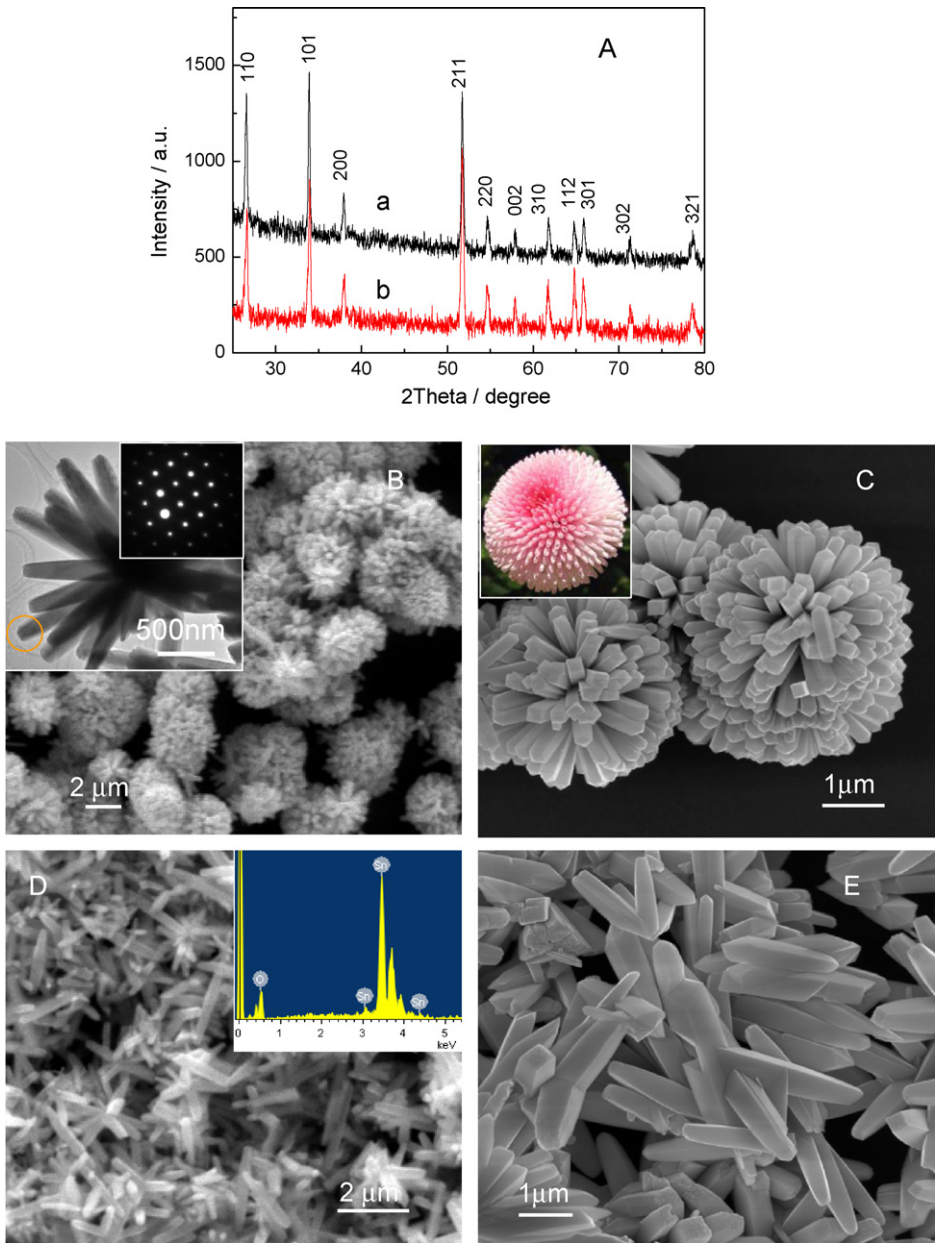

Fig. 1. XRD patterns (A) of SnO_2 nanoflowers (a) and SnO_2 nanorods (b). SEM image (B) and FESEM image (C) of SnO_2 nanoflowers, its SEAD pattern (the inset of B), and snow cone (the inset of C). SEM image (D) and FESEM image (E) of SnO_2 nanorods, and its EDS spectrum (the inset of D).

comparisons of the electrochemical performances on electrodes are shown in Table 1. Though the three electrodes have reached the same apparent geometric area, the Pt/SnO_2 flowers assembled by nanorods have much higher current density and larger working surface than other electrodes which is consist with the comparison of EAS. Compared with Pt/SnO_2 (rod), Pt/C and polycrystalline Pt nanocatalyst [17], we find that the Pt/SnO_2 (flower) electrocatalyst reveals not only tremendous current density of electrooxidation, but also lower onset potentials. Besides, the ratio of the forward scan peak current density (I_f) to the backward scan peak current density (I_b), I_f/I_b, can be used to describe the catalyst tolerance to carbonaceous species accumulation [17]. A higher ratio indicates preferable oxidation of alcohol to CO_2 during the forward scan and relatively less carbonaceous residues on the surface of the catalyst. In our electrochemical characterizations, the ratio was 1.27, 1.09, 0.87 and 0.93 for the Pt/SnO_2 (flower), Pt/SnO_2 (rod), Pt/C and polycrystalline Pt catalyst (Ref. [17]) in the methanol solution, respectively. While, the ratio was 1.21, 0.94, 0.78 and 0.80 for the

Table 1
Comparison of the performances of the two Pt/SnO_2/G electrodes and Pt/C/G electrode.

Electrodes	Peak potential (V)		Peak current density (mA mg_{Pt}^{-1})		I_f/I_b ratio	
	Methanol	Ethanol	Methanol	Ethanol	Methanol	Ethanol
Pt/SnO_2 (flower)/G	0.72	0.81	211.2	154.3	1.27	1.21
Pt/SnO_2 (rod)/G	0.72	0.75	69.8	29.6	1.09	0.94
Pt/C/G	0.71	0.82	107.8	58.7	0.87	0.78

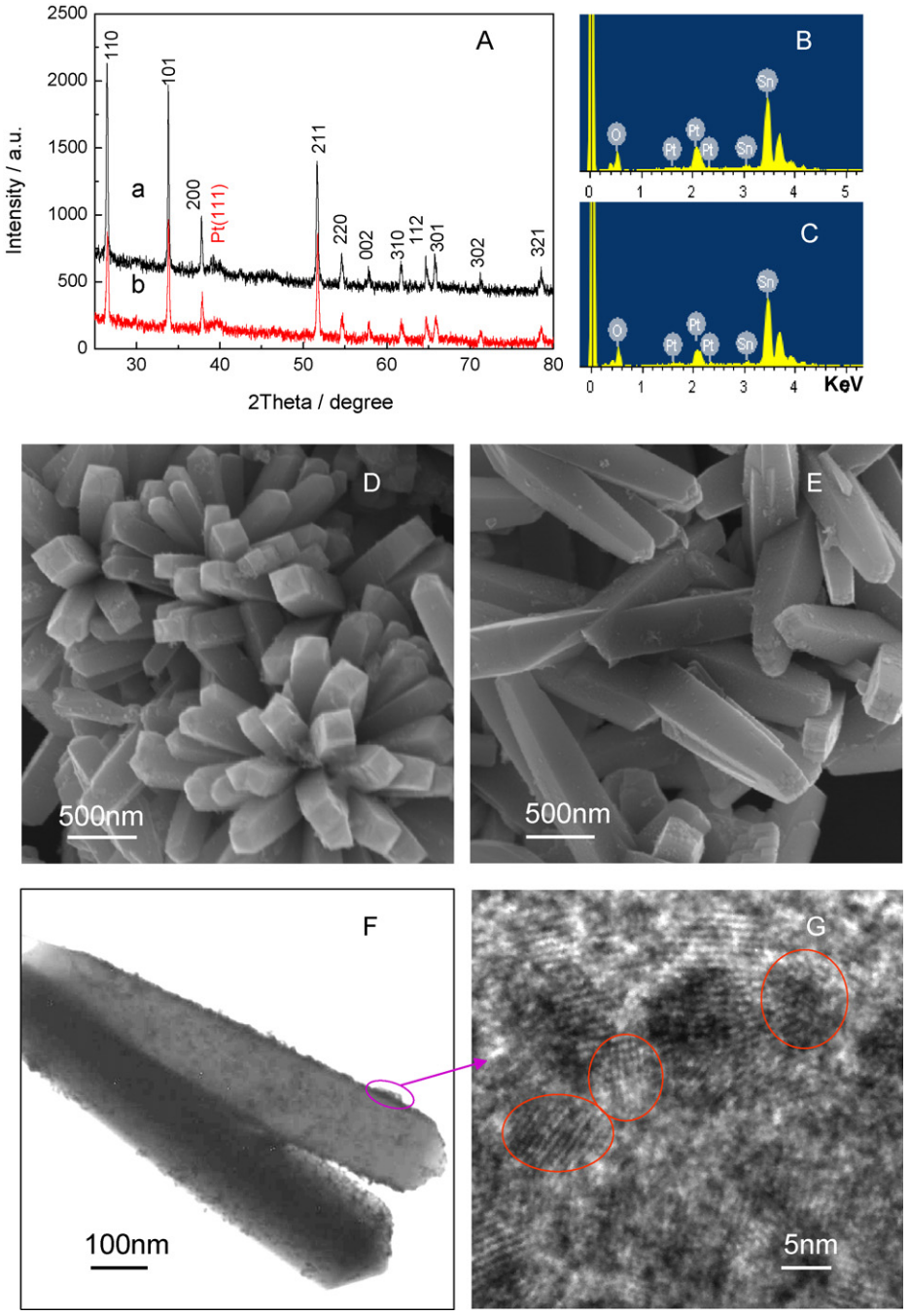

Fig. 2. XRD patterns (A) of Pt/SnO_2 (flower) catalyst (a) and Pt/SnO_2 (rod) catalyst (b). The corresponding EDS spectrums of Pt/SnO_2 (flower) (B) and Pt/SnO_2 (rod) (C). FESEM images of Pt/SnO_2 (flower) catalyst (D) and Pt/SnO_2 (rod) catalyst (E). TEM image of Pt/SnO_2 catalyst (F) and HRTEM image of Pt/SnO_2 catalyst (G).

Pt/SnO_2 (flower), Pt/SnO_2 (rod), Pt/C and polycrystalline Pt catalyst in the ethanol solution, respectively, as is shown in Table 1. This indicates the multidimensional structure of Pt/SnO_2 (flower) catalyst presents a perfect catalysis to electrooxidation of methanol and ethanol. However, the bare SnO_2/G electrode without Pt nanoparticles was also used for the alcohol oxidation, indicating no activity for alcohol oxidation (not shown), which is in good agreement with literature [18].

To further study the catalysis, LSVs at very slow potential scan rate of $5\,mV\,s^{-1}$ are conducted, as shown in Fig. 4. The peak current densities on the three electrodes for methanol and ethanol electrooxidation are in the order of Pt/SnO_2 (flower)/G > Pt/C/G > Pt/SnO_2 (rod)/G. Obviously, the Pt/SnO_2 (flower)/G electrode exhibits extremely high oxidation current density from these quasi-steady-state polarization curves. This suggests that the multidimensional structure of the Pt/SnO_2 (flower) catalyst can greatly enhance the electrocatalytic activity towards methanol and ethanol oxidation. The results observed here are in agreement with the CV studies.

The cause of the excellent catalysis to electrooxidation of methanol and ethanol of the Pt/SnO_2 (flower)/G electrode is the fact that Pt nanoparticles uniformly coat on the flowers and function as a multidimensional catalyst. But the Pt/SnO_2 (rod)/G and Pt/C/G electrode have less spatial structure. On the other hand, the radialized channels in the Pt/SnO_2 (flower) catalyst also improve the diffusion of liquid reactants into the catalyst layer and results in reduction of liquid sealing effect greatly. The reduction of liquid sealing effect in turn increases the active surface area for electro-

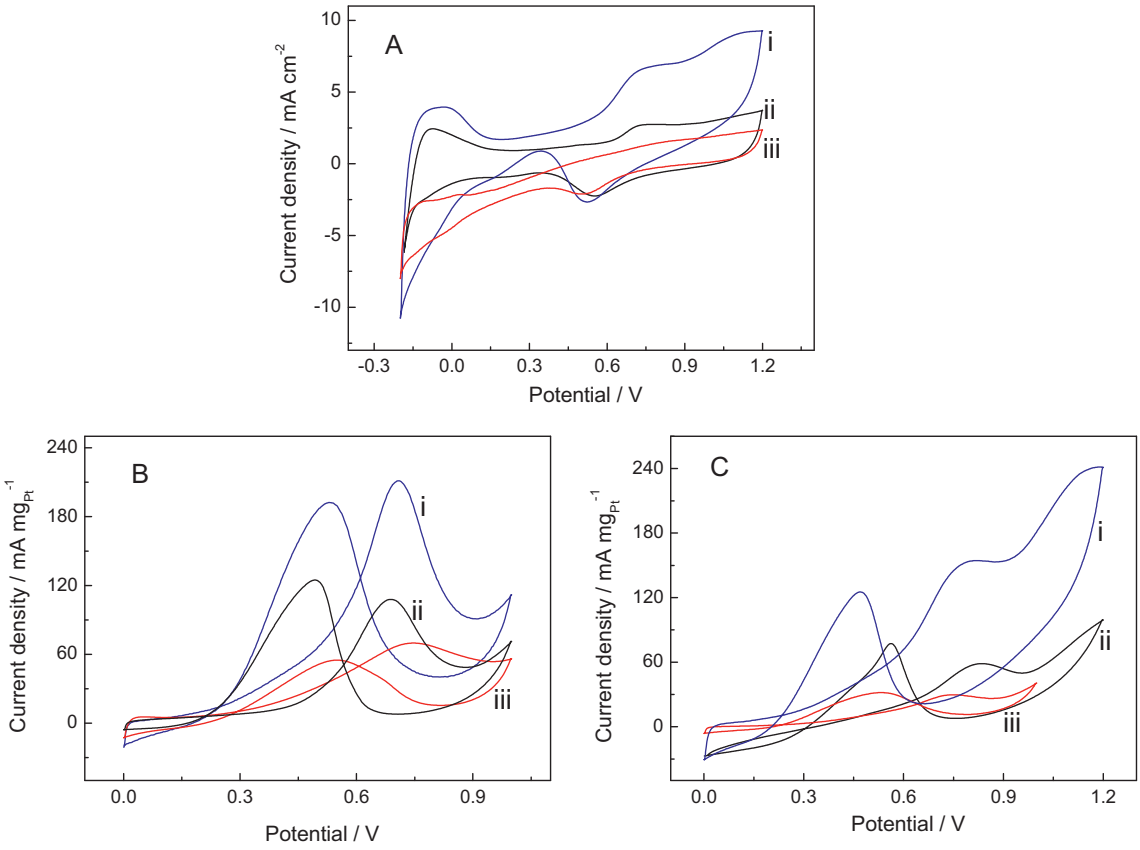

Fig. 3. CVs of Pt/SnO_2 (flower)/G (i), Pt/C/G (ii) and Pt/SnO_2 (rod)/G (iii) electrodes in 0.5 M H_2SO_4 (A), 0.5 M H_2SO_4 containing 1.0 M CH_3OH (B), or 1.0 M C_2H_5OH (C) with a sweep rate of 50 mV s^{-1}.

chemical reactions [19]. Furthermore, the CO tolerance of Pt can be improved by SnO_2 and the role of the oxide is proposed to relax the strong CO adsorption on Pt, which originates in the modification of electronic band structure of Pt and the interaction between Pt and the metal oxide [20].

The catalytic activities and stability of the Pt/SnO_2/G and Pt/C/G electrodes for methanol and ethanol electrooxidation have been investigated by chronoamperometries. In Fig. 5, a steady decrease in current is seen within the first few minutes for the three electrocatalysts, followed by a fairly constant current for longer time. Obviously, Fig. 5A and B reveals that the ultimate steady current density for methanol and ethanol electrooxidation on the Pt/SnO_2 (flower)/G electrode is 25.7 mA mg_{Pt}^{-1} and 24.7 mA mg_{P}^{-1}, respectively, which is higher than that on the Pt/C/G electrode (14.2 mA mg_{Pt}^{-1} and 10.0 mA mg_{Pt}^{-1}) and on the Pt/SnO_2 (rod)/G electrode (7.2 mA mg_{Pt}^{-1} and 4.1 mA mg_{Pt}^{-1}). Furthermore, the higher initial current means a greater number of active sites available for oxidation. It is demonstrated that the higher catalytic activity and better stability are achieved on the Pt/SnO_2 (flower)/G electrode for methanol and ethanol electrooxidation.

It is well known that the electrochemical impedance spectroscopy (EIS) technique is a powerful tool for characterizing the electrochemical processes occurring at the solution/electrode interface. Fig. 6 presents a typical electrochemical impedance spec-

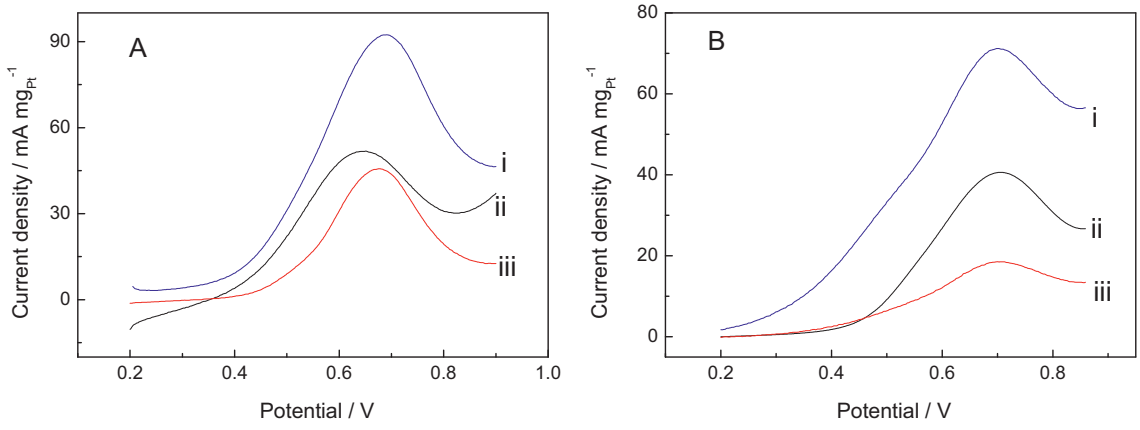

Fig. 4. LSVs of the Pt/SnO_2 (flower)/G (i), Pt/C/G (ii) and Pt/SnO_2 (rod)/G (iii) electrodes in 0.5 M H_2SO_4 containing 1.0 M CH_3OH (A) or 1.0 M C_2H_5OH (B) with a sweep rate of 5 mV s^{-1}.

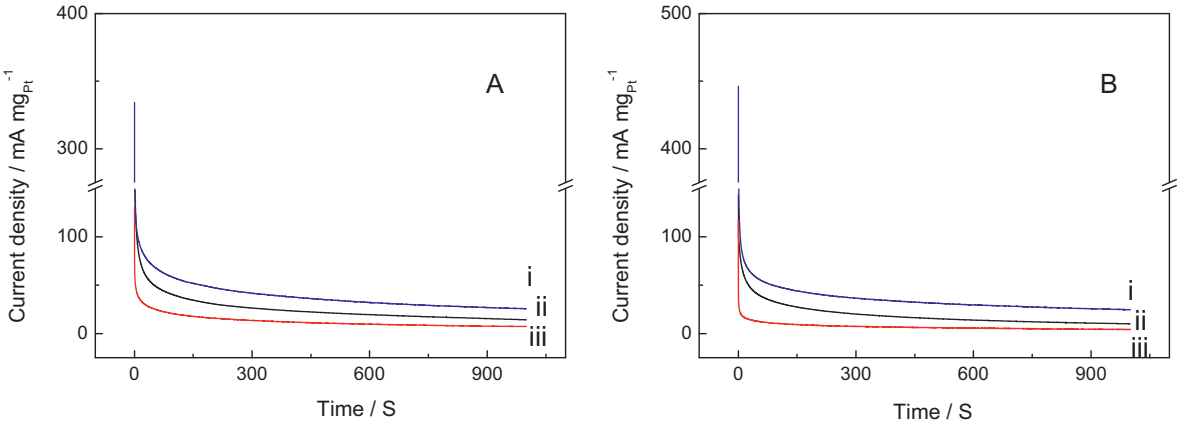

Fig. 5. Chronoamperometry diagrams of the Pt/SnO_2 (flower)/G (i), Pt/C/G (ii) and Pt/SnO_2 (rod)/G (iii) electrodes in 0.5 M H_2SO_4 containing 1.0 M CH_3OH (A) or 1.0 M C_2H_5OH (B) measured at 0.7 V for 1000 s.

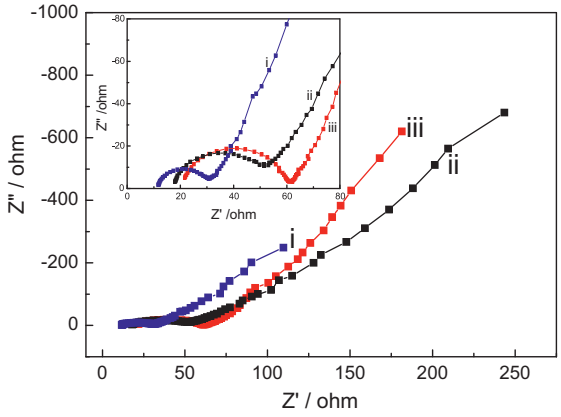

Fig. 6. Niquist plot of the Pt/SnO_2 (flower)/G (i), Pt/C/G (ii) and Pt/SnO_2 (rod)/G (iii) electrodes, and the magnified plot at high frequencies (inset).

trum in the form of a Nyquist plot of the Pt/SnO_2 (flower)/G, Pt/SnO_2 (rod)/G and Pt/C/G electrode in 0.1 M Na_2SO_4 at frequency ranging from 0.5 Hz to 100 kHz. The Nyquist plot includes a semicircle region lying on the Z'-axis observed at higher frequencies (it is related to the electron-transfer-limited process), followed by a linear part at lower frequencies (it is related to the diffusion-limited process). Usually, the semicircle diameter equals to the electron-transfer resistance, which is affected obviously by the surface modification of the electrode [21]. As shown in Fig. 6, the electron-transfer resistance of the Pt/SnO_2 (flower)/G electrode is less than that of the Pt/SnO_2 (rod)/G and Pt/C/G electrode, indicating that the multidimensional structure formed by the Pt/SnO_2 flowers can enhance the conductivity of the electrode owing to its faster interfacial charge carrier transfer as a result of higher ratio of surface to volume in comparison with the rod structure of Pt/SnO_2 and the nanoparticle structure of Pt/C. Usually, conductivity and surface activity are two important factors for a good analytical electrode [22,23]. As the Pt/SnO_2 flower structure not only provides the radial channels for a better diffusion of liquid reactants into the catalyst layer, but also retains faster electron-transfer speed on the interface between liquid and electrode. Therefore, the Pt/SnO_2 (flower)/G electrode possesses excellent performance in electrooxidation of methanol and ethanol.

4. Conclusions

Flower-shaped SnO_2 nanostructures and SnO_2 nanorods have been synthesized via the hydrothermal method. The multidimensional Pt/SnO_2 catalysts have been successfully obtained by uniform distribution of Pt nanoparticles on the SnO_2 flowers, which exhibit a highly catalytic oxidation activity to methanol and ethanol in acid solution. The series electrochemical measurements demonstrate that both the radial channels for a better diffusion of liquid reactants into the catalyst layer and faster electron-transfer on the interface between liquid and electrode are very important for the promotion of methanol and ethanol electrooxidation. Our investigations suggest that the Pt/SnO_2 (flower) electrocatalyst could be adopted as excellent catalyst in DAFCs.

Acknowledgments

This work has been funded by the NSFC (60976055), NSFDYS: 50925205, and Postgraduates' Science and Innovation Fund (201005B1A0010339) and Innovative Training Project (S-09109) of the 3rd-211 Project, and the large-scale equipment sharing fund of Chongqing University.

References

[1] H.S. Liu, C.J. Song, L. Zhang, J.J. Zhang, H.J. Wang, D.P. Wilkinson, J. Power Sources 155 (2006) 95–110.
[2] S.Q. Song, P. Tsiakaras, Appl. Catal. B 63 (2006) 187–193.
[3] J.M. Léger, J. Appl. Electrochem. 31 (2001) 767–771.
[4] W.S. Li, J. Lu, J.H. Du, D.S. Lu, H.Y. Chen, H. Li, Y.M. Wu, Electrochem. Commun. 7 (2005) 406–410.
[5] Z.L. Liu, L. Hong, S.W. Tay, Mater. Chem. Phys. 105 (2007) 222–228.
[6] F. Vigier, C. Coutanceau, F. Hahn, E.M. Belgsir, C. Lamy, J. Electroanal. Chem. 563 (2004) 81–89.
[7] J. Barranco, A.R. Pierna, J. Non-Cryst. Solids 354 (2008) 5153–5155.
[8] H.B. Yu, J.H. Kim, H.I. Lee, M.A. Scibioh, J. Lee, J. Han, S.P. Yoon, H.Y. Ha, J. Power Sources 140 (2005) 59–65.
[9] A. Kowal, S.L. Gojkovic, K.S. Lee, P. Olszewski, Y.E. Sung, Electrochem. Commun. 11 (2009) 724–727.
[10] X.Z. Cui, F.M. Cui, Q.J. He, L.M. Guo, M.L. Ruan, J.L. Shi, Fuel 89 (2010) 372–377.
[11] J.X. Wang, S.R. Brankovic, Y. Zhu, J.C. Hanson, R.R. Adzic, J. Electrochem. Soc. 150 (2003) A1108–A1117.
[12] L.H. Jiang, G.Q. Sun, S.G. Sun, J.G. Liu, S.H. Tang, H.Q. Li, B. Zhou, Q. Xin, Electrochim. Acta 50 (2005) 5384–5389.
[13] L.H. Jiang, G.Q. Sun, Z.H. Zhou, S.G. Sun, Q. Wang, S.Y. Yan, H.Q. Li, J. Tian, J.S. Guo, B. Zhou, Q. Xin, J. Phys. Chem. B 109 (2005) 8774–8778.
[14] W.Z. Hung, W.H. Chung, D.S. Tsai, D.P. Wilkinson, Y.S. Huang, Electrochim. Acta 55 (2010) 2116–2122.
[15] X.S. He, C.G. Hu, H. Liu, Catal. Commun. 12 (2010) 100–104.
[16] A. Pozio, M. De Francesco, A. Cemmi, F. Cardellini, L. Giorgi, J. Power Sources 105 (2002) 13–19.
[17] S.B. Han, Y.J. Song, J.M. Lee, J.Y. Kim, K.W. Park, Electrochem. Commun. 10 (2008) 1044–1047.
[18] M.S. Saha, R. Li, X. Sun, Electrochem. Commun. 9 (2007) 2229–2234.
[19] F.Y. Xie, Z.Q. Tian, H. Meng, P.K. Shen, J. Power Sources 141 (2005) 211–215.

[20] T. Matsui, K. Fujiwara, T. Okanishi, R. Kikuchi, T. Takeguchi, K. Eguchi, J. Power Sources 155 (2006) 152–156.
[21] X.X. Zhong, J.H. Chen, B. Liu, Y. Xu, Y.F. Kuang, J. Solid State Electrochem. 11 (2007) 463–468.
[22] C.G. Hu, W.L. Wang, K.J. Liao, G.B. Liu, Y.T. Wang, J. Phys. Chem. Solids 65 (2004) 1731–1736.
[23] C.G. Hu, Y.Y. Zhang, G. Bao, Y.L. Zhang, M.L. Liu, Z.L. Wang, Chem. Phys. Lett. 418 (2006) 524–529.